

# Object reconstruction from a single architectural image taken with an uncalibrated camera

Frank A. van den Heuvel

## *Summary:*

*This paper reports on a line-photogrammetric approach for modelling architectural objects using a single image. For the estimation of the object model parameters a least-squares bundle adjustment is developed. In addition to the manually derived image line observations several constraints on the object parameters are incorporated in the adjustment. Coplanarity, parallelism, and perpendicularity are examples of these constraints. The constraints improve the quality of the estimated object parameters and reduce the number of image line observations required. This paper concentrates on the extreme case where the number of images required for reconstruction is reduced to one.*

*The interior orientation parameters of the single image are determined in a separate least-squares adjustment. The mathematical model of this adjustment is based on parallelism and perpendicularity constraints on image line observations that are extracted using a line-growing algorithm. These constraints result from a vanishing point detection procedure. With successful vanishing point detection the determination of the parameters of the interior orientation does not require manual interaction.*

*As an example, the approach is applied for the reconstruction of part of a demolished building using a single image from the Meydenbauer archives. The interior orientation of the image was unknown. It is concluded that the approach is very suitable for this type of imagery and results in a partial reconstruction of which the precision is assessed.*

## **1 Introduction**

The research reported in this paper concentrates on object modelling in architectural photogrammetry. The main goal is to exploit the characteristics of this application in order to allow object modelling from a minimum number of images, and assess the quality of the resulting object model. The latter is especially important when redundancy is low which is even more likely to occur when only a single image is used. However, in architectural photogrammetry sufficient object information can generally be inferred from the image for an estimation of the object model parameters with considerable redundancy. This holds true, even for reconstruction from a single image, as is illustrated by the example presented in section 4.

The main characteristic of the application is the availability of object information that results from knowledge or assumptions on the construction of the building. The object information applied in the approach presented in this paper is split into three groups:

1. Object edges are straight. When lens distortion is absent, straight object edges result in straight line features in the image. Especially in architectural photogrammetry line features show advantages over point features for measurement (Streilein, 1998; van den Heuvel, 2000). Therefore, only line features are used as photogrammetric observations.

2. Object faces are planar. In fact, this type of object information relates to the previous type as the intersection of two planar faces leads to a straight edge. This object information implies that a polyhedral boundary representation or B-rep is a suitable type of representation for the object at hand. In this representation the object edges and faces intersect in the object points. To ensure a valid B-rep, object constraints are used that force the points into the planes.
3. Object shape constraints. The main constraints used are:
  - Parallelism of object edges and faces
  - Perpendicularity of object edges and faces
  - Coplanarity of object points and faces
  - Symmetry of object edges

Control points, i.e. object points with known co-ordinates, are not required, other than a minimum set for defining a co-ordinate system. It is possible to include known distances between two points or between two parallel planes.

The use of a priori object information as outlined above distinguishes this approach from other ones. Here, the term line-photogrammetry is applied because the line features in the images are the observations. However, there is no explicit parameterisation for the edges in object space as in many other line-photogrammetric approaches (Mulawa & Mikhail, 1988; Zielinski, 1993; Patias et al., 1995; Schwermann, 1995). The main reasons for not using object line parameters are the large number of object constraints required for a valid B-rep, in combination with the complexity of the formulation of these and other object constraints.

Assumptions on the shape of the building are applied in the reconstruction in the form of weighted constraints. The need for object constraints also results from the use of a polyhedral B-rep for model representation. The so-called point-in-plane constraint (section 4.1) ensures planar faces. Other methods refrain from the use of shape constraints and therefore these methods require multiple images (Streilein, 1998) or an image sequence (Pollefeys et al., 2000).

Object reconstruction from measurements in a single image is frequently investigated by researchers from the computer vision community (Bräuer-Burchardt & Voss, 1999; Guillou et al., 2000; Jelinek & Taylor, 1999; Liebowitz et al., 1999; Sturm & Maybank, 1999), and less in the photogrammetric community (Williamson & Brill, 1990; Braun, 1994; Karras & Petsa, 1999). The International Committee for Architectural Photogrammetry (CIPA) established a task group on the topic (CIPA-TG2, 2001). All methods use at least parallelism and perpendicularity information of edges in object space. Sometimes edge detectors are used to extract the line features in the image. However, manual interaction is often required, especially for the extraction of edges needed for object reconstruction. It is beyond the scope of this paper to discuss the differences between the various approaches. The main difference of the approach presented in this paper and approaches found in the literature is the application of a rigorous least-squares adjustment for the parameter estimation for the camera calibration as well as for the object reconstruction. This adjustment facilitates error propagation and simplifies the assessment of the quality of the results.

The line-photogrammetric bundle adjustment for multiple images was developed a few years ago (van den Heuvel, 1999a). The application of this bundle adjustment to line observations in a single image is new. For single image bundle adjustment the approximate value computation for the object parameters needs special attention (section 4.2). The main reason is that the parameters

cannot be approximated by forward intersection with two or more images. Furthermore, new object shape constraints are implemented.

Previous research on single image object reconstruction concentrated on the adjustment of condition equations that contain no object parameters (van den Heuvel, 1998b). Object reconstruction (i.e. the computation of the parameters of the object model) was done in a separate step using the adjusted image line observations and object constraints. This approach does not result in a unique solution for the object model in all cases. Another disadvantage is that error propagation is cumbersome due to the separate object reconstruction step. Therefore, the quality of the object model cannot be assessed as with a weighted bundle adjustment with parameters. Furthermore, the object constraints in the form of condition equations on the line observations are complex for many types of constraints. However, its advantage is that approximate values for object parameters are not required.

The rest of this paper is structured as follows. Section 2 gives an overview of the method. The camera calibration from a single image is presented in section 3, and the object reconstruction in section 4. The method is applied to a scanned reproduction from the Meydenbauer archives. The results are discussed in sections 3.3.3 and 4.3. Conclusions are drawn in section 5.

## 2 Overview of the method

The developed method for object reconstruction from a single image with unknown interior orientation consists of two main steps (Figure 1). The first step is a highly automated procedure for the least-squares estimation of the interior orientation parameters including lens distortion. The mathematical model is built from parallelism and perpendicularity object constraints on straight edges in the image. The edges are extracted using a line-growing algorithm. The constraints result from a vanishing point detection procedure that also does not require manual interaction.

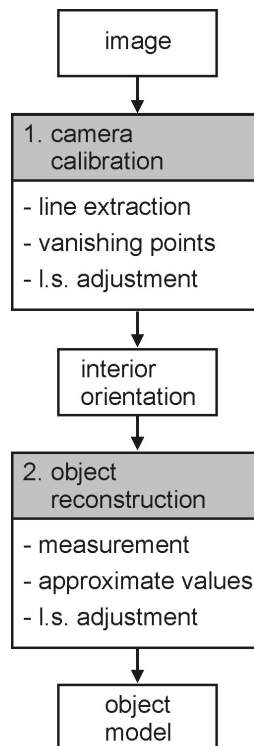


Figure 1. Overview of the procedure for single image object reconstruction

In the second step manual measurements are required to extract edges in the image that correspond to object edges. Furthermore, object information such as topology and shape constraints is to be inferred from the image. After computation of approximate values, a bundle adjustment is used to adjust the line observations and estimate the parameters of the object model, and the exterior orientation. Interior orientation parameters from the first step are not estimated in the latter adjustment because high correlations with the exterior orientation parameters would deteriorate the solution, and is even likely to prohibit convergence of the iterative procedure. Furthermore, it is not expected that the precision of the interior orientation parameters can be improved in the second step, assuming a correct constraint specification by the vanishing point detection procedure. The types of object constraints used in the first step are also used in the second step, supplemented with other types of object constraints such as symmetry constraints. However, the image line observations are different in both steps.

### **3 Camera calibration**

In the first step of the procedure the interior orientation parameters of the single image are determined from edges extracted using image processing. Section 3.1 deals with the edge extraction and the representation of an edge in the mathematical model. In section 3.2 the vanishing point detection method is discussed. This can be regarded as a procedure for grouping edges that have the same orientation in space. This information is used for the formulation of condition equations that build the mathematical model. The estimation of the interior orientation parameters using this model is discussed in section 3.3.

#### **3.1 From edge extraction to observations**

In the approach presented here, lines in the image plane serve as observations in the mathematical models, and not points as in conventional photogrammetry. The method for line extraction is briefly discussed in the next section. The parameterisation of the image lines and the options for the stochastic model are presented in the sections thereafter.

##### **3.1.1 Edge extraction by line-growing**

Edges are automatically extracted by applying a line-growing algorithm that is summarised as follows. The line-growing process starts at seed points in the image where the gradient is above a pre-set threshold. The algorithm searches in the direction indicated by the gradient for pixels that sufficiently match the seed point pixel in gradient strength and orientation. The neighbouring pixels that match the criteria are added to the pixels of the line. A line is fitted to the gathered pixels and the growing process is continued. When no more pixels can be added to the line, the resulting fitted line - specified by its endpoints - is checked against a pre-set minimum line length. The number and length of extracted straight image lines depends on the parameters such as the minimum gradient strength and the minimum line length.

For the estimation of the interior orientation parameters only lines extracted with this line-growing algorithm are used. No manual measurements are required.

##### **3.1.2 The interpretation plane**

A straight line in the image can be parameterised in several ways. Although two parameters suffice for the representation of an image line, the four image co-ordinates  $(x, y)$  of the end points

are used here. This guarantees a singularity-free representation, and simplifies the formulation of the stochastic model.

Like a point in the image is associated with a ray in space, a line in the image is associated with a plane in space. This plane is called the interpretation plane (Figure 2).

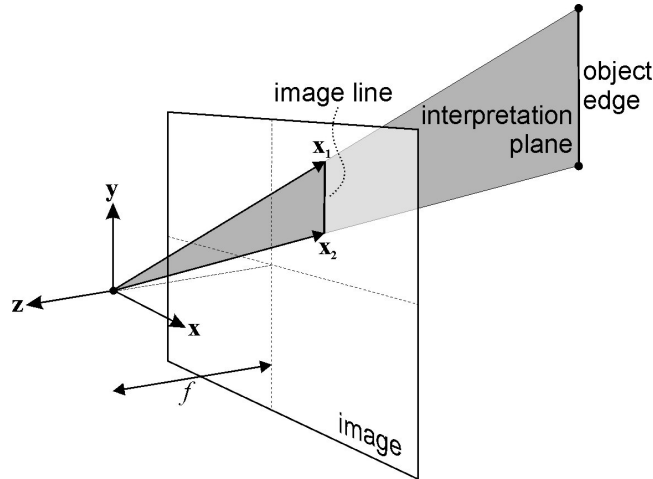


Figure 2. A line in the image and its associated interpretation plane

Assume a perfect central projection with the principal point in the centre of the image, and focal distance  $f$ . The orientation of the interpretation plane is defined by its normal vector ( $\mathbf{n}$ ) that is constructed from the two vectors from the projection plane centre to the endpoints of the line ( $\mathbf{x}$ ):

$$\mathbf{n} = \mathbf{x}_1 \times \mathbf{x}_2, \text{ with: } \mathbf{x} = (x, y, -f) \quad (1)$$

The calibration procedure is started with a rough approximation for the focal length.

### 3.1.3 The stochastic model

The stochastic model plays an important role in the quality assessment of the parameters estimated by a weighted least-squares adjustment. To set up the covariance matrix ( $\mathbf{Q}$ ) of the observations two options have been implemented:

1. The variances of the co-ordinates of the endpoints decrease linearly with the length of the line in pixels.
2. The variance is constant for all endpoint co-ordinates.

The first model is designed for lines extracted using an edge detection approach. The second model is used for lines that are extracted manually by measurement of their endpoints. For the tests described in this paper only the latter model is applied.

### 3.1.4 Example

Figure 3 shows the image that is used to illustrate the methods presented in this paper. It is a low resolution scan ( $1200 \times 865$  pixels) of a reproduction of a photograph by Albrecht Meydenbauer taken in the year 1911. It depicts a building in the historical centre of Berlin called “Kommandantur”. This building no longer exists like many other buildings in the historical centre. There is a need for reconstruction using the photographs from the Meydenbauer archives such as this one (Wiedeman et al., 2000). In Figure 3 (right) the lines extracted using the line-growing algorithm presented in section 3.1.1 are overlaid with the image. The extraction was

limited to the part of the image that contains the building. 223 lines were extracted with the minimum line length set to 40 pixels.

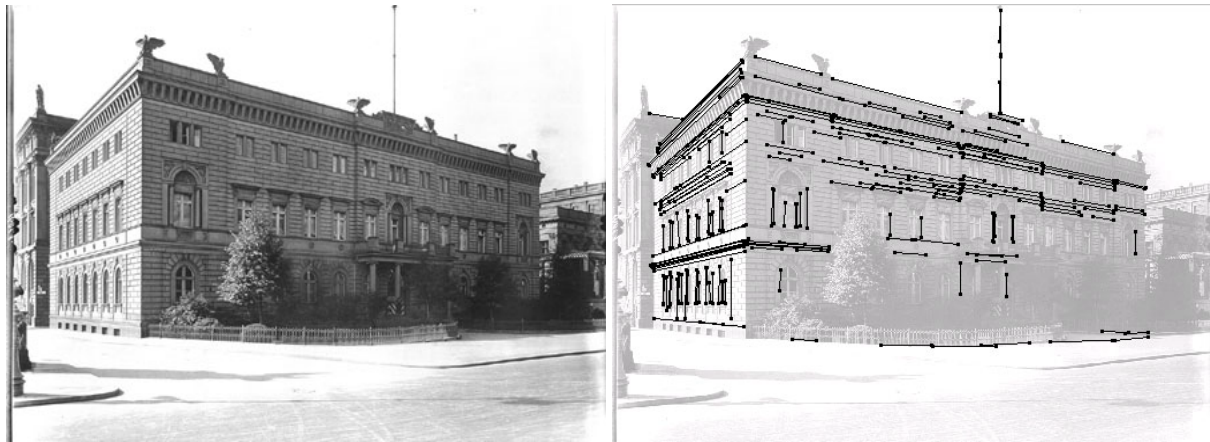


Figure 3. The Meydenbauer image (left) and the automatically extracted image lines (right).

### 3.2 Vanishing point detection

When straight image lines have been extracted the parameters of interior orientation are determined by applying two types of object constraints. First, parallelism assumptions of object edges are applied. Second, perpendicularity is used of the three major object orientations defined by three groups of parallel edges. When lens distortion is absent, the projections of object edges that are parallel intersect in a point in the image called the vanishing point (Figure 4). With the detection of a vanishing point the parallelism of the related object edges is assumed.

The method for vanishing point detection was designed to make use of the assumption of perpendicularity between the three main object orientations (van den Heuvel, 1998a). However, when principal point and effective focal length are unknown only parallelism assumptions can be used in the vanishing point detection procedure. Projections of parallel object edges intersect in a vanishing point independent of the location of the principal point or the focal length. The perpendicularity assumption is introduced to allow the estimation of the interior orientation parameters (section 3.3).

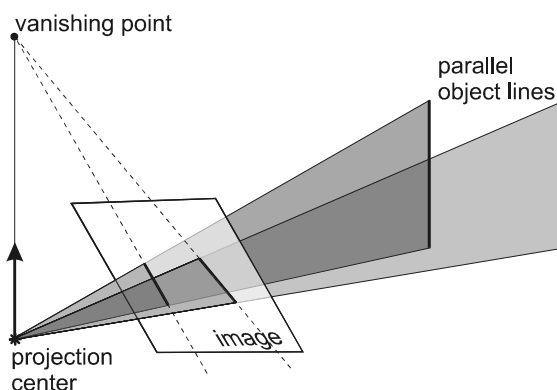


Figure 4. Vanishing point as the intersection of the projections of parallel lines in object space

### 3.2.1 Intersection of three interpretation planes

The method for vanishing point detection is based on the statistical testing of the intersection hypotheses of combinations of three image lines, or rather the intersection of the three interpretation planes associated with these lines. The intersection constraint can be written as the determinant of the matrix built from the three normal vectors ( $\mathbf{n}$ ) of the interpretation planes  $i, j$ , and  $k$ :

$$[\mathbf{n}^i, \mathbf{n}^j, \mathbf{n}^k] = \det(\mathbf{n}^i, \mathbf{n}^j, \mathbf{n}^k) = 0 \quad (2)$$

In case the lines do not (perfectly) intersect this constraint will result in a misclosure ( $m$ ):

$$[\mathbf{n}^i, \mathbf{n}^j, \mathbf{n}^k] = m \quad (3)$$

The hypothesis of interpretation plane intersection is tested with the normalised misclosure relative to a critical value ( $cv$ ):

$$\left| \frac{m}{\sigma_m} \right| < cv \quad (4)$$

The standard deviation of the misclosure ( $\sigma_m$ ) is computed from the covariance matrix of the image co-ordinates ( $\mathbf{Q}$ ) (section 3.1.3):

$$\sigma_m^2 = \mathbf{b}^T \mathbf{Q} \mathbf{b} \quad (5)$$

with  $\mathbf{b}$  the vector of partial derivatives. The part of  $\mathbf{b}$  for image point  $a$  can be written as:

$$\mathbf{b}^a = \frac{\partial m}{\partial \mathbf{n}^i} \frac{\partial \mathbf{n}^i}{\partial \mathbf{x}^a} \quad (6)$$

### 3.2.2 The procedure for vanishing point detection

The procedure for the detection of the vanishing points is summarised as follows:

- The longest of all available image lines is chosen as the first line of the vanishing point.
- The test values of all combinations of this longest line and two other image lines are computed according to (4).
- Lines are clustered using the results of the testing. This usually results in several clusters that often have a large number of lines in common.
- For the largest clusters an adjustment is set up, based on all (independent) constraints in the cluster and a line error hypothesis is tested for each line.
- Rejected lines are removed from the clusters and the adjustment is repeated until all remaining lines are accepted.
- The cluster with the largest number of lines is selected as the first vanishing point cluster.

The procedure is repeated with the remaining (non-clustered) lines to detect the other two vanishing points. More details on this procedure are found in (van den Heuvel, 1998a).

### 3.2.3 Example

The result of the vanishing point detection procedure applied to the extracted lines of the Meydenbauer image is shown in Figure 5. The left most image corresponds to the first vanishing point and contains the longest line (264 pixels). A few lines of this vanishing point do not correspond to object edges with the same orientation, but were not removed. All extracted lines

were assigned to one of the three vanishing points. The number of lines of the first, second, and third vanishing point is respectively 117, 42, and 64. Note that the third vanishing point is at infinity in the image plane. In other words, the image is in a two-point perspective (Williamson & Brill, 1990). In the current implementation, the interior orientation parameters are input to the procedure. It has been verified that the vanishing point detection is not affected by a change in these parameters. With an a priori standard deviation of 1 pixel (constant value for the endpoint co-ordinates of an image line) the estimated variance factor of the adjustment of all parallelism constraints is 0.576.



Figure 5. Result of detection of three vanishing points.

### 3.3 Interior orientation parameter estimation

#### 3.3.1 The mathematical model with parameters

To build the mathematical model for the least-squares parameter estimation two types of constraints are applied, i.e. parallelism and perpendicularity constraints. The constraints are specified automatically using the vanishing point detection algorithm described in the previous section. There, only the parallelism constraint is used and the mathematical model does not contain parameters. Now the model is extended with the interior orientation parameters and (1) becomes:

$$\mathbf{x} = \begin{pmatrix} x - x_o - k_1(x - x_o)r^2 \\ y - y_o - k_1(y - y_o)r^2 \\ -f \end{pmatrix} \quad (7)$$

with:

$f$ : effective focal length

$x_o, y_o$ : co-ordinates of the principal point

$k_1$ : radial lens distortion parameter

$$r^2 = (x - x_o)^2 + (y - y_o)^2$$

If required, lens distortion can be modelled more extensively.

The perpendicularity constraints involve the interpretation plane normals of four lines, consisting of two perpendicular sets (1 and 2) of two lines that are parallel in object space. This constraint can be written as:

$$(\mathbf{n}_1^i \times \mathbf{n}_1^j) \cdot (\mathbf{n}_2^k \times \mathbf{n}_2^l) = 0 \quad (8)$$

In order to set up a least-squares adjustment, equations (2) and (8) are linearised with respect to both the parameters and the observations. This leads to a so-called mixed model (Teunissen, 1999):

$$\mathbf{B}^T E\{\mathbf{y}\} = \mathbf{A} \mathbf{x} ; \mathbf{Q}_y \quad (9)$$

with:

$E\{.\}$  expectation operator

$\mathbf{y}$  vector of the observations (observed – computed)

$\mathbf{x}$  vector of corrections to the parameters

$\mathbf{A}, \mathbf{B}$  design matrices (partial derivatives)

$\mathbf{Q}_y$  covariance matrix of the observations (section 3.1.3)

The constraints used for the model (9) have to be independent in order to compute the solution as described in the next section. This is achieved in the following way. First, for each object orientation the two image lines are selected that best define the object orientation. Let us call these two lines the *base* lines. Then for each of the  $n-2$  remaining lines of that orientation, parallelism constraints are set up according to (2) ( $n$  is the number of lines in a cluster of parallel lines). Each constraint involves three lines, two of which are the base lines. In this way,  $n-2$  independent constraints are defined for each object orientation. Second, only three perpendicularity constraints are set up according to (8). These constraints are formulated using the base lines of each object orientation that have been used for the parallelism constraints as well. The three independent constraints define perpendicularity between three combinations of two object axes ( $XY$ ,  $YZ$ , and  $ZX$ ).

### 3.3.2 Parameter estimation

The system of equations (9) is transformed into a standard system of observations equations by the introduction of the so-called derived observations ( $\mathbf{z}$ ):

$$E\{\mathbf{z}\} = \mathbf{A} \mathbf{x} ; \mathbf{Q}_z \quad (10)$$

with:

$$E\{\mathbf{z}\} = \mathbf{B}^T E\{\mathbf{y}\} ; \mathbf{Q}_z = \mathbf{B}^T \mathbf{Q}_y \mathbf{B}$$

The full covariance matrix  $\mathbf{Q}_z$  of the derived observations results from propagation of the diagonal covariance matrix of the observations  $\mathbf{Q}_y$ . The least-squares solution to the system (10) is well known:

$$\hat{\mathbf{x}} = (\mathbf{A}^T \mathbf{Q}_z^{-1} \mathbf{A})^{-1} \mathbf{A}^T \mathbf{Q}_z^{-1} \mathbf{z} \quad (11)$$

The computation of the residuals of the original observations is explained in (van den Heuvel, 1999a).

Since the mathematical model is non-linear in both the parameters and the observations, the iteration process needs special attention. Convergence has to be obtained by iterating in the parameters first to avoid a solution that is biased by the approximate values of the parameters. After that, iteration in both the parameters and the observations leads to a set of parameters and observations that fit the model.

In the presence of considerable lens distortion the solution is to be computed in two steps (van den Heuvel, 1999b). In the first step the lens distortion is estimated. In the second step the interior orientation parameters are estimated using the results of the first step.

### 3.3.3 Example

The procedure for estimation of interior orientation parameters is applied to the Meydenbauer image, using the results of the vanishing point detection for the specification of the parallelism and the three perpendicularity constraints. Trying to estimate the three interior orientation parameters using the adjusted observations from the vanishing point detection, a correlation of close to a 100% between the focal length and the principal point  $x$  co-ordinate appears. This is due to the two-point perspective (section 3.2.3). Fixing the principal point in the middle of the image in column direction, the estimation of the two remaining parameters converged in five iteration steps. Convergence is not sensitive to the approximate values. For both parameters starting values were more than 150 pixels different from the solution presented in Table 1. Formal standard deviations are based on the a priori standard deviation of 1 pixel for the endpoints of the image lines. Using the original line observations the estimated variance factor is 0.588 (218 degrees of freedom), close to the value of the vanishing point adjustment (section 3.2.3). Estimation of the radial lens distortion parameter  $k_1$  results in a value of  $0.30 \times 10^{-3}$ , only 2.5 times its standard deviation.

Interior orientation (pixels)	original observations		adjusted observations	
	Parameter	Standard deviation	Parameter	Standard deviation
Principal point $y$	586	12.3	601	12.8
Focal length	1131	10.7	1152	9.4

Table 1. Estimated interior orientation parameters (in pixels).

## 4 Object reconstruction

The line-photogrammetric bundle adjustment was developed for the estimation of the parameters of a boundary representation from the image line observations of multiple images (van den Heuvel, 1999a). In this section, first an overview of the line-photogrammetric bundle adjustment is presented (section 4.1). Approximate values for the parameters are required because of the non-linearity of the model. Especially in the case of single image processing, approximate value computation needs special attention (section 4.2). The application of the presented bundle adjustment procedure on the Meydenbauer image is discussed in section 4.3.

### 4.1 Overview of the line-photogrammetric bundle adjustment

The mathematical model of the line-photogrammetric bundle adjustment relates the image line observations (section 3.1) to the parameters of the object model. Although usually only the coordinates of the points represent the geometry of a B-rep, in this approach also the parameters of the object planes are incorporated in the model. The reason is the simplicity of the formulation of geometric object constraints. Two groups of parameters can be distinguished:

- 1 object model parameters (points and planes)
- 2 exterior orientation parameters

Interior orientation parameters are not estimated and have to be determined beforehand (section 3).

Over-parameterisation is applied in combination with constraints to avoid singularities inherent in some parameter choices. Four parameters are used for each object plane, i.e. the normal vector of the plane and a position parameter. The position is the perpendicular distance of the plane to

the origin. A constraint is used to force the normal vector length to 1. The rotation matrix of exterior orientation is parameterised by four parameters of a quaternion. The length of the vector of the quaternion elements is constrained to 1.

The basic relation of the line-photogrammetric bundle adjustment is the point-in-plane constraint. First, there is an *object point in interpretation plane* constraint (Figure 6). Second, the *object point in object plane* constraint is formulated that is very similar to the first one.

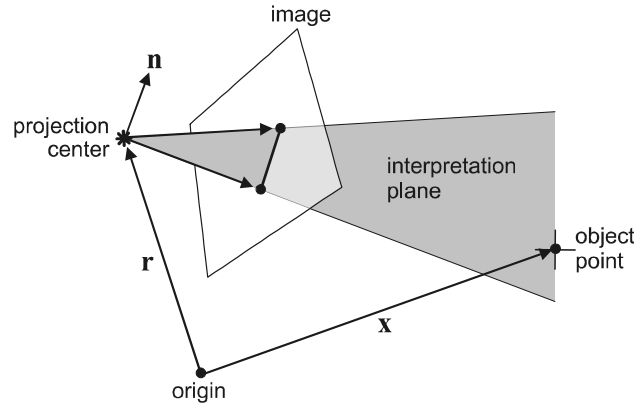


Figure 6. Object point in interpretation plane.

For the object point in interpretation plane constraint the normal vector to the interpretation plane is rotated into the object co-ordinate system by applying the rotation matrix of exterior orientation ( $\mathbf{R}$ ), and (1) becomes for line  $i$ :

$$\mathbf{n}_i = \mathbf{R} (\mathbf{x}_1 \times \mathbf{x}_2) \quad (12)$$

With the vector to the projection centre ( $\mathbf{r}$ ) and the vector to the object point ( $\mathbf{x}$ ), the object point in interpretation plane constraint for image line  $i$  is written as:

$$\mathbf{n}_i \cdot \mathbf{x} - \mathbf{n}_i \cdot \mathbf{r} = 0 \quad (13)$$

With the (signed) plane position parameter  $l_i$  the object point in object plane constraint becomes:

$$\mathbf{n}_i \cdot \mathbf{x} - l_i = 0 \quad (14)$$

Equation (13) relates the observations to the object point parameters, while (14) relates the object point parameters to the object plane parameters. With more than three points in a plane, the latter constraint enforces coplanarity of object points. It is important to note that object faces that are coplanar share the same plane parameters.

A number of object shape constraints have been implemented that will not be discussed in detail here. In (Hrabacek & van den Heuvel, 2000) the formulation of most of them is presented:

- Points: coplanarity (14), distance between two points, and co-ordinates of control points.
- Lines: parallelogram, symmetry constraint (section 4.2).
- Planes: angle, parallelism, and distance between two planes.

All constraints have been implemented as weighted observation equations. This has the advantage that realistic weights can be used for instance for the shape constraints, and thus uncertainty in the constraints is taken into account. Furthermore, constraints do not have to be independent. The relations that build the mathematical model are non-linear in the parameters and non-linear in the observations. The least-squares solution to this model is discussed in section 3.3.

## 4.2 Measurement and approximate value computation

Only a few of the lines extracted using the line-growing algorithm described in section 3.1.1 are suitable for object modelling and correspond to the edges of the building façades. Many other edges show poor contrast in the image. Therefore, manual interaction is required. Not only for line measurement, but also for the specification of the topology of the B-rep, and object shape constraints.

Approximate values of all parameters have to be available to set up the linearised observation equations. With the image line measurements, object topology, and shape constraints available, the approximate values are computed in the following order:

- 1 Exterior orientation parameters
- 2 Object point parameters
- 3 Object plane parameters

The last two steps are then repeated until no new parameters are computed.

In the first step the direct solution that is presented in (van den Heuvel, 1997) is used to compute the exterior orientation parameters based on the measurement of 4 points (or lines) that correspond to a rectangle in object space. For the second step all available linear equations that contain the object co-ordinates are gathered. These equations relate to the following constraints:

- *Point in interpretation plane.* The exterior orientation parameters as well as the interpretation plane normals are regarded as constants and thus equation (13) becomes linear in the object point co-ordinates.
- *Point in object plane.* When step 2 is repeated, object plane parameters are available from step 3. Regarding them as constants, also (14) becomes linear in the co-ordinates.
- *Control point co-ordinates.* These linear equations are of the form  $\mathbf{x} - \mathbf{x}_c = 0$ , where  $\mathbf{x}_c$  is the vector of control point co-ordinates.
- *Parallelogram equations.* These equations relate the four corner points of a parallelogram in object space, and have the simple linear form  $(\mathbf{x}_1 - \mathbf{x}_2) - (\mathbf{x}_3 - \mathbf{x}_4) = 0$ .

Apart from the control point constraint, all these constraints are independent of the choice of the co-ordinate system. This is not the case for the symmetry constraint. This constraint has the same form as the parallelogram constraint, apart from the fact that the vector  $(\mathbf{x}_3 - \mathbf{x}_4)$  is mirrored with respect to the XY, YZ, or XZ plane. In the current implementation this constraint is only used for object reconstruction.

The computation of approximate plane parameters is based on (14) only. Then the point co-ordinates from step 2 are treated as constants, and (14) is linear in the plane parameters. Plane parameters can be computed when the co-ordinates of at least three points are available. Similarly, object point co-ordinates can be computed when three or more planes are available. These planes can be interpretation planes as well as object planes.

## 4.3 Example

In Figure 7 the manual measurements are overlaid on the Meydenbauer image. Closed polygons are measured through their corner points of which the image co-ordinates are stored. Each corner point is an endpoint of at least two individual image lines and relates to one point in object space. Each closed polygon is associated with an object face and each image line with an interpretation

plane (Figure 2). In this way the topology of the polyhedral B-rep is specified together with the relations between image measurements and object points.

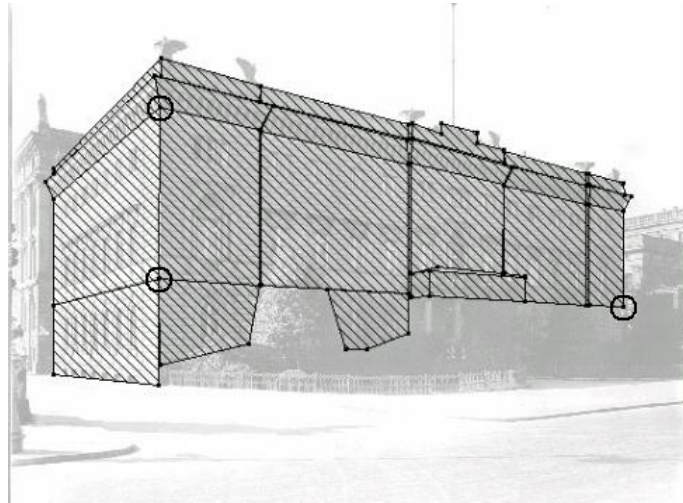


Figure 7. Manually measured points, lines, and faces.

In this approach only object parts (parts of building faces) that are visible in the image are reconstructed. As in the multiple image example described in (van den Heuvel, 1999a), some occluded object parts can be reconstructed with only one image also, but this has not been investigated here.

	number	parameters	equations	precision ( $\sigma$ )
image lines	100	-	152	$\mathbf{Q}_z$ (10)
distance	1	-	1 (control)	0.1m
object points	76	228	6 (control)	0.001m
object planes	12	48	12	$10^{-6}$
image orientation	1	7	1	$10^{-6}$
point-in-plane	-	-	123	0.01m
plane angles	11	-	11	0.1deg
parallelogram	15	-	45	0.01m
symmetry	6	-	18	0.01m
<b>totals</b>		<b>283</b>	<b>369</b>	

Table 2. Parameters and equations in the adjustment.

In Table 2 the number of image and object features, and the related number of parameters and equations are listed. This table also contains an overview of the object constraints that were inferred from the image and the precision that was assigned to them. Although 29 faces were specified, for only 12 planes there are parameters in the model. In this way coplanarity of several faces is enforced. In Figure 7 three control points are indicated by circles. Six co-ordinates of these points have been fixed. The distance between the two points on the front of the building was derived from a cadastral map (41.39m), and processed as a distance constraint. In this way the co-ordinate system is fixed with minimum control. The estimated variance factor is 0.535 with an a priori standard deviation for the endpoints of the lines of 1 pixel (86 degrees of freedom). The formal standard deviations of the object co-ordinates (excluding control points) are summarised in Table 3. Note that the standard deviations depend on the control point choice, and

the applied shape constraints and their weights. The largest residual to an endpoint co-ordinate is 2.0 pixel. Reliability parameters are not computed. However, it is noted that for some observations there is no redundancy and thus reliability is absent.

Standard deviation (m)	X	Y	Z
Average	0.080	0.095	0.055
Minimum	0.013	0.008	0.022
Maximum	0.135	0.384	0.127

Table 3. Precision of the object points ( $\sigma$  in meter).

The estimated exterior orientation parameters show that the photograph was taken at a distance of 34.5m ( $\sigma$  0.17m) from the corner of the building at a height of 1.78m ( $\sigma$  0.08m) above the lowest (ground) points of the object model.

The determined boundary representation is converted to VRML-format with textures derived from the image by a rectification for each face. Two views of the resulting object model are shown in Figure 8. The error ellipsoids are enlarged with a factor 10 relative to the model and visualise the covariance matrices of the object points. The model is available on the Internet (Meydenbauer, 2001).

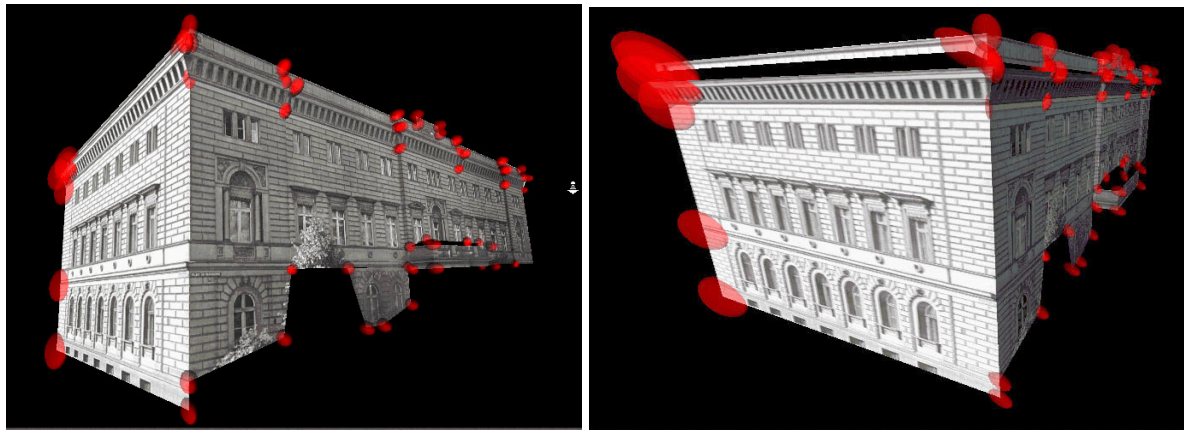


Figure 8. Two views on the texture mapped model (error ellipsoids enlarged with a factor 10).

## 5 Conclusions

Methods are presented for camera calibration and object reconstruction from line measurements in a single image. No manual measurements are required for the procedure for camera calibration when vanishing point detection is successful. The parameters of interior orientation are estimated in a least-squares adjustment from image lines extracted by line-growing. The mathematical model is built with independent constraint equations that are non-linear in the parameters as well as in the observations. A vanishing point detection algorithm infers the constraints. Applying the calibration procedure to a historical image of a building, the position of the principal point could not be estimated in column direction due to the two-point perspective. Estimation in row direction showed the principal point is more than 150 pixels below the centre of the image. The formal precision of the principal point is 12 pixels ( $1\sigma$ ). The precision of the focal length is 11 pixels.

In the procedure for object reconstruction the point and plane parameters of a B-rep are estimated together with the parameters of exterior orientation using a line-photogrammetric bundle

adjustment. The adjustment model is built from point-in-plane constraint equations that relate the image line measurements to the object co-ordinates, and the co-ordinates to the plane parameters. Furthermore, the topology of the B-rep and several object shape constraints are incorporated in the least-squares adjustment through weighted observation equations. Adjustment of 100 image lines (standard deviation of endpoints set to 1 pixel) and 32 shape constraints resulted in the 3D co-ordinates of 76 points with an average precision between 5 and 10 cm.

The paper demonstrates the potential of a single image with unknown interior and exterior orientations for partial reconstruction of architectural objects. All parameters involved are estimated using a least-squares adjustment that facilitates the assessment of their precision. If available, more images with possibly different interior orientations can be included in the adjustment. A more complete reconstruction of higher quality will be the result.

## References

IAPRS - International Archives of Photogrammetry and Remote Sensing

Braun, C., 1994: Interpretation and correction of single line drawings for the reconstruction of objects in space. ISPRS Commission III, Munich, Vol. 2357, 85-90.

Bräuer-Burchardt, Ch., K. Voss, 1999: Monocular 3D-reconstruction of buildings. In: Girod B, Niemann H and Seidel HP (eds.): VMV '99, Infix, 109-116.

CIPA-TG2, 2001: [http://info.uibk.ac.at/sci-org/cipa/tg2\\_1.html](http://info.uibk.ac.at/sci-org/cipa/tg2_1.html), accessed May 14, 2001.

Guillou, E., D. Meneveaux, E. Maisel, K. Bouatouch, 2000: Using vanishing points for camera calibration and coarse 3D reconstruction from a single image. *The visual computer*, Springer, Vol. 16, 396-410.

Heuvel, F.A. van den, 1997: Exterior Orientation using Coplanar Parallel Lines. 10th Scandinavian Conference on Image Analysis, Lappeenranta, 71-78.

Heuvel, F.A. van den, 1998a: Vanishing point detection for architectural photogrammetry. IAPRS, Hakodate, Vol. 32 part 5, 652-659.

Heuvel, F.A. van den, 1998b: 3D reconstruction from a single image using geometric constraints. *ISPRS Journal of Photogrammetry and Remote Sensing*, Vol.53, No.6, 354-368.

Heuvel, F.A. van den, 1999a: A Line-photogrammetric mathematical model for the reconstruction of polyhedral objects. *Videometrics VI*, 28-29 Jan. 99, San Jose, Proceedings of SPIE, Vol. 3641, 60-71.

Heuvel, F.A. van den, 1999b: Estimation of interior orientation parameters from constraints on line measurements in a single image. IAPRS, Thessaloniki, Vol. 32 (5W11), 81-88.

Heuvel, F.A. van den, 2000: Line-photogrammetry and its application for reconstruction from a single image. 19. Jahrestagung der DGPF, Essen, Publikationen der Deutschen Gesellschaft für Photogrammetrie und Fernerkundung, Vol. 8, 255-263.

Hrabacek, J., F.A. van den Heuvel, 2000: Weighted geometric object constraints integrated in a line-photogrammetric bundle adjustment. IAPRS, Amsterdam, Vol. 33, Part B5, 380-387.

Jelinek, D., C.J. Taylor, 1999: Reconstruction of linearly parameterized models from single images with a camera of unknown focal length. *CVPR'99*, Fort Collins, Vol. 2, 346-352.

Karras, G.E., E. Petsa, 1999: Metric information from uncalibrated single images. *Proceedings XVII CIPA Symposium October 99*, Recife/Olinda, Brazil.

Liebowitz, D., A. Criminisi, A. Zisserman, 1999: Creating architectural models from images. Eurographics'99, Vol. 18, 3, 39-50.

Meydenbauer, 2001: <http://www.geo.tudelft.nl/frs/architec/Meydenbauer/>, accessed May 14, 2001.

Mulawa, D.C., E.M. Mikhail, 1988: Photogrammetric treatment of linear features. IAPRS, Vol. 27, part B10, 383-393.

Patias, P., E. Petsa, A. Streilein, 1995: Digital Line Photogrammetry. IGP Bericht 252, ETH Zürich.

Pollefeys, M., R. Koch, M. Vergauwen, L. van Gool, 2000: Automated reconstruction of 3D scenes from sequences of images. ISPRS Journal of Photogrammetry & Remote Sensing, Elsevier, Vol. 55, 4, 251-267.

Schwermann, R., 1995: Geradengestuetzte Bildorientierung in der Nahbereichs-photogrammetrie. Veröffentlichung des Geodetischen Institutes der RWTH Aachen, Vol. 52.

Streilein, A., 1998: Digitale Photogrammetrie und CAAD. Dissertation Nr. 12897, ETH Zuerich.

Sturm, P.F., S.J. Maybank, 1999: A method for interactive 3D reconstruction of piecewise planar objects from single images. BMVC 10th British Machine Vision Conference, Nottingham, England, 265-274.

Teunissen, P.J.G., 1999: Adjustment Theory – an Introduction. Delft University Press, Delft, ISBN 90-407-1974-8.

Wiedemann, A., M. Hemmleb, J. Albertz, 2000: Reconstruction of historical buildings based on images from the Meydenbauer archives. IAPRS, Amsterdam, Vol. 33, part B5, 887-893.

Williamson, J. R., M.H. Brill, 1990: Dimensional analysis through perspective - a reference manual. ASPRS, ISBN 0-8403-5673.

Zielinski, H., 1993: Object Reconstruction with Digital Line Photogrammetry. Dissertation Royal Institute of Technology, Sweden.

### **Address**

Ir. Frank A. van den Heuvel, Delft University of Technology, Geodesy Department,  
Thijssseweg 11, NL-2629JA Delft,

Tel. +31-15-278 7609, Fax +31-15-278 2745

E-mail: [F.A.vandenHeuvel@geo.tudelft.nl](mailto:F.A.vandenHeuvel@geo.tudelft.nl)